

# Polarized neutron reflection used to characterize cobalt/copper multilayers

W. Schwarzacher and W. Allison

*Cavendish Laboratory, Department of Physics, Cambridge University, Cambridge CB3 0HE, United Kingdom*

J. Penfold and C. Shackleton

*Neutron Science Division, S.E.R.C. Rutherford-Appleton Laboratory, Didcot OX11 0QX, United Kingdom*

C. D. England, W. R. Bennett, J. R. Dutcher, and C. M. Falco

*Department of Physics and Optical Sciences Center, University of Arizona, Tucson, Arizona 85721, U.S.A.*

(Received 5 July 1990; accepted for publication 11 December 1990)

The polarized neutron reflectivity (PNR) of cobalt/copper multilayer films has been measured close to the critical edge for total reflection. Prominent features in the scattered neutron intensity, such as the superlattice diffraction peaks and the positions of the critical edge for total reflection, are sensitive to both the magnetic and structural properties of films, making PNR a useful tool for the characterization of magnetic metallic superlattices. The films were prepared by sputter deposition and the sample composition was measured by Rutherford backscattering spectroscopy. It has been found that while the density of the sputtered copper/cobalt multilayers is approximately 5% less than the bulk metals, the cobalt magnetic dipole moment per atom is little changed compared to the bulk. Evidence is also found for oxidation of the top cobalt layers.

## I. INTRODUCTION

Spin-dependent scattering of neutrons occurs when the neutron refractive index of a magnetic material contains a spin-dependent part. Thus one can study the magnetization profile of a sample normal to its surface by measuring its neutron reflectivity  $R$  for neutrons polarized parallel ( $R+$ ) and antiparallel ( $R-$ ) to the magnetization direction.<sup>1</sup> In this paper we show how this technique may be applied to the study of magnetic superlattices and demonstrate that it can provide valuable information on both the magnetic and compositional structure of such materials. In particular, we report the results of a polarized neutron reflection study of cobalt/copper multilayer films prepared by vacuum sputter deposition and show that while the density of the film components is reduced by  $\sim 5\%$  compared to the bulk metals, the cobalt magnetic dipole moment remains close to its bulk value.

The magnetic properties of metal/metal superlattices in which one of the components is a magnetic transition metal are of particular interest. For example, Katayama, Awano, and Nishihara<sup>2</sup> observed a strong enhancement of the polar magneto-optic Kerr rotation angle in cobalt/copper and iron/copper multilayers as a function of increasing superlattice repeat distance for wavelengths close to the Cu absorption edge ( $\lambda \approx 560$  nm). A further stimulus to the study of magnetic metal superlattices was the recent discovery that the resistance of superlattices consisting of alternate layers of iron and chromium could change significantly in the presence of a magnetic field.<sup>3,4</sup>

Since neutrons are scattered both magnetically and via the nuclear force, neutron scattering can provide information about both the magnetic and compositional structure of a sample and is therefore ideally suited to the structural and magnetic characterization of magnetic metal superlat-

tices. Pioneering work of this kind was carried out by Sato *et al.*<sup>5</sup> who studied the interface magnetism of Fe/SiO and Ni/SiO multilayered films, and Felcher *et al.*<sup>6</sup> who studied the magnetization of a compositionally modulated alloy of nickel and copper. More recently, polarized neutron diffraction has been used by Majkrzak to investigate magnetic coupling in single-crystal rare-earth superlattices<sup>7</sup> and by Majkrzak, Axe, and Böni to investigate the interface magnetism of Fe/Ge multilayered films.<sup>8</sup>

What distinguishes the work presented here is the emphasis on measuring the reflectivity close to the critical edge for total reflection where it is necessary to use a neutron-optics approach to fit the data. It will be seen that such measurements can provide information, not only about the superlattice periodicity, but also about the film/substrate and film/air interfaces and about the average composition and magnetization of the film.

## II. SAMPLE PREPARATION

Polycrystalline cobalt/copper multilayers were deposited on single-crystal sapphire substrates using magnetically enhanced direct current triode sputtering guns. The sputtering rate could be held constant to within  $\pm 0.1\%$  and to grow a superlattice in which the thicknesses of the cobalt layers  $d_{\text{Co}}$  and the thicknesses of the copper layers  $d_{\text{Cu}}$  were constant the substrate was exposed to the sources for each metal in turn for fixed lengths of time. The base pressure of this diffusion-pumped system is  $\sim 1 \times 10^{-7}$  Torr and it has been shown that such a system is capable of depositing many metals with purity equivalent to the starting target material.<sup>9</sup>

After growth  $N_M$ , the number of atoms of each species  $M$  per unit area of the film was measured using Rutherford backscattering spectroscopy (RBS). The RBS values of

$N_M$  were accurate to within  $\pm 3\%$  and could be used to estimate the total thickness of  $M$  present,  $D_M$  by using

$$D_M = N_M / \rho_M, \quad (1)$$

if  $\rho_M$ , the number density of  $M$ , is assumed equal to its bulk value,  $d_M$  could be calculated from  $D_M$  since the number of repeat units in the superlattice was known. The polarized neutron reflection measurements, in which a diffraction peak corresponding to the superlattice repeat distance is seen, were used to check this value of  $d_M$  and hence whether or not the assumption that  $\rho_M$  was equal to its bulk value was correct.

Initial structural characterization of the multilayer films was carried out using x-ray diffraction. The multilayer periodicity was confirmed by small-angle x-ray-diffraction patterns which showed a diffraction peak corresponding to the superlattice repeat distance as observed subsequently in the polarized neutron reflection experiments, while x-ray measurements at larger angles gave information on the structure of the film components. The films were found to have a strong fcc copper[111]/hcp cobalt[0001] texture.<sup>10</sup>

The polycrystalline nature of the sputtered films will not affect the neutron reflectivity, which is only sensitive to structure on a scale of tens of Å. However, we would expect the polarized neutron reflectivity to be sensitive to interfacial roughness which we might expect to be greater for a sputtered film than an epitaxial film.

### III. NEUTRON REFLECTIVITY CALCULATIONS

A convenient starting point for the calculation of neutron reflectivity is temporarily to ignore the complications introduced by factors such as the interfacial roughness. The assumption of a superlattice with flat and completely sharp interfaces between successive layers allows the reflectivity to be determined using methods analogous to those of conventional multilayer optics.<sup>11</sup> Each layer of material  $M$  may be described by a characteristic transfer matrix which relates the neutron wave function  $\Psi_I$  and its derivative  $\Psi'_I$  at the upper boundary to the corresponding values  $\Psi_{II}$  and  $\Psi'_{II}$  at the lower boundary:

$$\begin{pmatrix} \Psi_I \\ \Psi'_I \end{pmatrix} = \begin{pmatrix} \cos q_M d_M & - (1/q_M) \sin q_M d_M \\ q_M \sin q_M d_M & \cos q_M d_M \end{pmatrix} \begin{pmatrix} \Psi_{II} \\ \Psi'_{II} \end{pmatrix}. \quad (2)$$

In Eq. (2),  $d_M$  is the layer thickness and  $q_M$  is the perpendicular component of the incident neutron wave vector in  $M$ .  $q_M$  is given by

$$q_M^2 \approx q_0^2 - 4\pi\rho_M (\bar{b}_M \pm Cm_M), \quad (3)$$

where  $q_0$  is the perpendicular component of the incident neutron wave vector in the vacuum,  $\rho_M$  is the number density of  $M$ , and  $C$  is a constant  $\approx 2.70 \times 10^{-15}$  m. The term involving the mean nuclear scattering length ( $\bar{b}_M$ ) is due to scattering by the nuclear force while the term containing the average magnetic dipole moment per atom ( $m_M$ , measured in Bohr magnetons) arises from the magnetic scattering. The sign of  $Cm_M$  is positive for neutrons polarized with their spin parallel to the sample magnetiza-

tion and negative for neutrons polarized antiparallel to the sample magnetization.

By multiplying the transfer matrices for the different layers comprising the superlattice together, it is possible to calculate  $T$ , the transfer matrix describing the complete multilayer film. From the elements  $t_{ij}$  of this matrix and a knowledge of  $q_s$ , the perpendicular component of the neutron wave vector in the substrate, it is possible to calculate the polarized neutron reflectivities  $R_+$  and  $R_-$  using

$$R_{\pm} = \left| \frac{iq_1 t_{11\pm} - q_1 q_3 t_{12\pm} - t_{21\pm} - iq_3 t_{22\pm}}{iq_1 t_{11\pm} - q_1 q_3 t_{12\pm} + t_{21\pm} + iq_3 t_{22\pm}} \right|^2. \quad (4)$$

The condition for a superlattice diffraction peak to occur at a particular  $q_0$  is the familiar Bragg condition, which may be written as

$$2q_{Co} d_{Co} + 2q_{Cu} d_{Cu} = 2n\pi \quad (5)$$

for the cobalt/copper system. Using Eq. 3, this may be rewritten as

$$2[q_0^2 - 4\pi\rho_{Co}(b_{Co} \pm Cm_{Co})]^{1/2} d_{Co} + 2(q_0^2 - 4\pi\rho_{Cu}b_{Cu})^{1/2} d_{Cu} = 2n\pi. \quad (6)$$

When  $q_0$  becomes very large,  $q_0 \approx q_{Co} \approx q_{Cu}$  but close to the critical edge the distinction between them is important.

Another relationship between  $d_{Co}$ ,  $d_{Cu}$ ,  $\rho_{Co}$ ,  $m_{Co}$ , and  $\rho_{Cu}$  may be obtained from the position of the critical edge  $q_c$  which is the value of  $q_0$  at which  $q$  in the superlattice equals zero and the film becomes totally reflecting. To a good approximation  $q_c$  is given by

$$q_c^2 = 4\pi(\rho b)_{\text{mean}} = 4\pi \left( \frac{\rho_{Co}(b_{Co} \pm Cm_{Co})d_{Co} + \rho_{Cu}b_{Cu}d_{Cu}}{d_{Co} + d_{Cu}} \right). \quad (7)$$

From Eq. (7) it is clear that the critical edge for the film is different for the spin-parallel and spin-antiparallel cases. In the case of a multilayer film on a semi-infinite substrate there is one further complication that arises because the critical edge for the composite system will be determined by the medium with the greatest scattering density. If the scattering density of the substrate is greater than the mean scattering density of the film then the substrate scattering density will determine the position of the critical edge. For the cobalt/copper multilayers in the present work the scattering properties of the multilayer film determined the critical edge for spin-parallel neutrons while the sapphire substrate determines the critical edge for spin-antiparallel neutrons.

### IV. EXPERIMENTAL RESULTS

The polarized neutron reflection measurements were made using the polarized neutron mode of the time-of-flight reflectometer CRISP<sup>12</sup> at the Rutherford-Appleton Laboratory pulsed neutron source ISIS. This instrument is shown schematically in Fig. 1. A cobalt/titanium supermirror which selectively reflects spin-parallel neutrons is used to polarize the incident neutron beam with an effi-

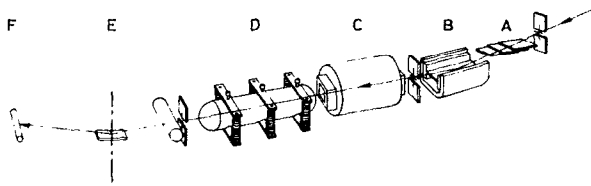


FIG. 1. Schematic diagram of CRISP in its polarized neutron mode. The frame-overlap mirrors are labeled A, B is the cobalt-titanium polarizing supermirror, C is the Drabkin two-coil non-adiabatic spin flipper, D is the guide field, E is the incident beam monitor, F is the sample position and G is the main detector.

ciency of  $\sim 99.50\%$ , and the beam polarization may be reversed using a Drabkin two-coil nonadiabatic spin flipper.<sup>13</sup>

The neutron reflectivity of a material is a function of  $q_0$ , the component of the incident neutron wave vector perpendicular to the sample surface. This quantity may be varied by varying either the incident neutron wavelength  $\lambda$  or the neutron angle of incidence  $\theta$  since  $q_0$  is given by

$$q_0 = (2\pi/\lambda)\sin\theta, \quad (8)$$

On CRISP we measure the reflectivity as a function of wavelength at a particular angle of incidence. Spin-parallel and antiparallel reflectivities were measured for two different gazing angles of incidence,  $\theta \approx 0.45^\circ$  and  $1.0^\circ$  in order to extend the  $q_0$  range covered. Since the scattering density of sapphire is known and this determines  $q_c$  for the spin-antiparallel critical edge, by measuring the wavelength at which this critical edge occurs, it is possible to use Eq. (8) to determine  $\theta$  more precisely.

Two multilayer samples were studied, each consisting of eight repeat units of copper/cobalt on a single-crystal sapphire substrate with the copper deposited first and the cobalt last. Sample C146 had  $d_{\text{Cu}} = 146\text{\AA}$  and  $d_{\text{Co}} = 72\text{\AA}$ , while sample C29 had  $d_{\text{Cu}} = 29\text{\AA}$  and  $d_{\text{Co}} = 73\text{\AA}$ . The quoted thicknesses are those obtained by Rutherford backscattering spectroscopy assuming bulk densities. Measurements were carried out at room temperature and the multilayer samples were mounted on a goniometer between the poles of an electromagnet that gave a coercive field of approximately 3.0 kG in the plane of the film.

Figure 2(a) shows the measured neutron reflectivities for sample C146 as a function of wavelength for an angle of incidence of  $7.77 \times 10^{-3}$  rad ( $\approx 0.45^\circ$ ), the solid lines being the calculated reflectivities assuming the quoted thicknesses, bulk densities, and bulk (hcp) cobalt magnetic moment ( $1.7 \mu_B$ ). The most prominent features in the reflectivity profiles are the first-order superlattice diffraction peak (A) in the spin-antiparallel scattering and the critical edges (B). Fringes due to the overall thickness of the film are also evident (C). The superlattice diffraction peak in the spin-parallel data is very weak because the spin-parallel neutrons see little contrast between cobalt and copper.

A comparison of the experimental data points and calculated reflectivities in Fig. 2(a) shows that the calculated

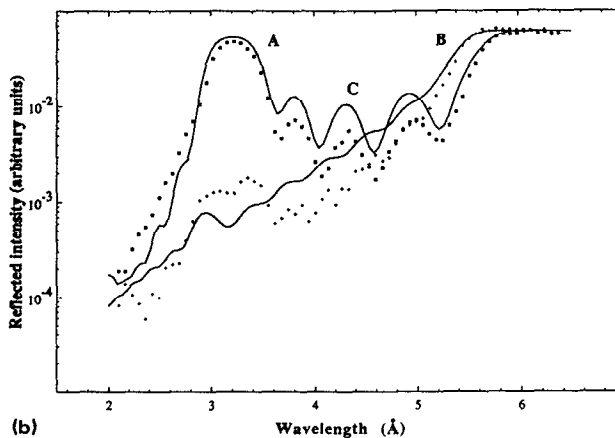
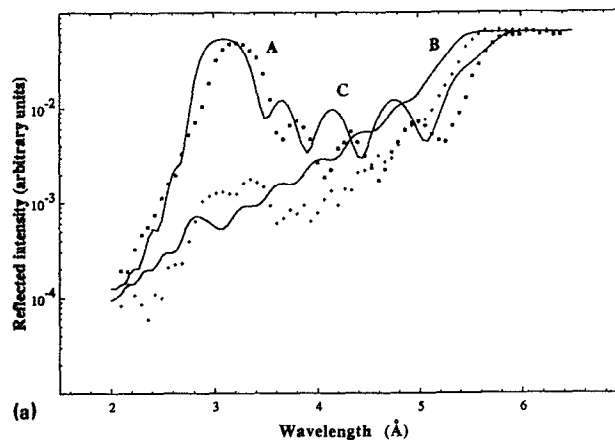


FIG. 2. (a) The measured neutron reflectivities for the spin-parallel (crosses) and spin-antiparallel (squares) configurations with sample C146 (nominally eight repeat units of 146 Å copper and 72 Å cobalt). The curves are the calculated reflectivities assuming the quoted thicknesses, bulk densities and bulk hcp cobalt magnetic dipole moment  $1.7 \mu_B$ . The angle of incidence was  $\sim 0.45^\circ$  and the effective angular resolution was assumed to be  $\sim 2\%$ . Using these parameter the wavelength calculated for the spin-antiparallel superlattice peak A and the spin-parallel critical edge B are too low. (b) As in (a), expected that the calculated reflectivities were calculated with thicknesses increased by 4% (to 152 Å copper and 75 Å cobalt) while the bulk densities were reduced by 4% (to  $8.1 \times 10^{28}$  and  $8.7 \times 10^{28}$  atoms/m<sup>3</sup>, respectively). This choice of parameters is much more successful in reproducing the positions of the spin-antiparallel superlattice peak A and the spin-parallel critical edge B.

positions of the diffraction peak and the spin-parallel critical edge are incorrect. The fact that the superlattice diffraction peak is found at a greater than predicted wavelength implies that the true superlattice period is larger than we assumed, while the fact that the wavelength of the spin-antiparallel critical edge is greater than predicted implies that the film scattering density is less than we assumed.

An improved fit to the data is obtained if we relax the assumption that the superlattice components have bulk densities. For Fig. 2(b), the copper and cobalt densities ( $\rho_{\text{Cu}}$  and  $\rho_{\text{Co}}$ ) and the corresponding layer thicknesses ( $d_{\text{Cu}}$  and  $d_{\text{Co}}$ ) have been varied subject to the constraint that  $\rho_{\text{Cu}}d_{\text{Cu}}$  and  $\rho_{\text{Co}}d_{\text{Co}}$  are as determined by Rutherford backscattering measurements. A  $4 \pm 1\%$  reduction in den-

sity of both components reproduces the observed position of the spin-antiparallel diffraction peak and subsidiary peaks as well as the position of the spin-parallel critical edge rather well, providing confirmation of x-ray-diffraction measurements, which suggest a reduction of  $5 \pm 3\%$  in the average density of similar films.<sup>10</sup> The fact that such good agreement with the experiment can be obtained at the spin-parallel critical edge using the bulk value of the cobalt magnetic dipole moment also suggests that any departure of the film magnetic dipole moment from the bulk value is small.

So far we have improved the agreement between calculation and experiment by varying magnetic and structural parameters while assuming an ideal superlattice. Now we demonstrate how the fit may be refined by taking into account secondary structural properties such as the interfacial roughness that one would expect in a system grown by sputter deposition. There are two types of rough interface that must be considered: The first occurs between each copper and cobalt layer, while the second type occurs in the topmost cobalt layer, which is exposed to air and will exhibit some degree of roughness as well as some degree of oxidation. Roughness between the copper and cobalt layers will reduce the reflectivity at both the spin-antiparallel first-order diffraction peak [A in Fig. 2(b)] and the fringes due to the overall film thickness (C) but not the height of the fringes relative to the first-order diffraction peak. The relative height of the fringes will, however, be affected by oxidation at the interface of the topmost cobalt layer with the atmosphere. Any roughness at the interface between film and substrate may be neglected as there is little difference in the scattering density of copper and sapphire.

It is possible to model a rough interface by allowing the scattering density to vary smoothly from one material to the next.<sup>14</sup> However, the same effect can be obtained with a much simpler computational procedure that involves a single buffer layer of intermediate scattering density.<sup>15</sup> Introducing a buffer layer of increasing thickness is equivalent to decreasing the sharpness of the interface. Thus the basic superlattice unit of one cobalt and one copper layer can be replaced by a unit cell including two buffer layers, as shown schematically in Fig. 3(a). Once the thickness of the buffer layer  $d_{\text{buff}}$  is chosen, the thicknesses of the remaining copper and cobalt layers are determined by the requirement that the superlattice repeat distance is unchanged.

In a similar way the topmost cobalt layer also requires two buffer layers: one between the metallic cobalt and its oxide and a second between the oxide and air [Fig. 3(b)]. Bogen and Küppers<sup>16</sup> found that when polycrystalline cobalt was exposed to oxygen at 300 K approximately 10 monolayers of cobalt were oxidized. Lee *et al.*<sup>17</sup> found that when Co(0001) was exposed to oxygen at 300 K the oxide formed was CoO and so the scattering density of bulk CoO was used for the oxide layer. CoO is antiferromagnetic at low temperatures and so, unlike pure cobalt, its refractive index is not spin-dependent.

As a final refinement to the calculated intensity profiles we have allowed for the possibility of partial depolarization

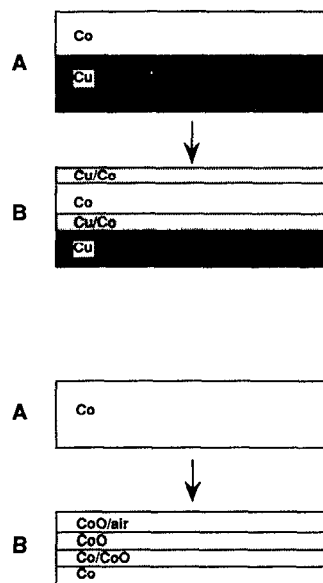


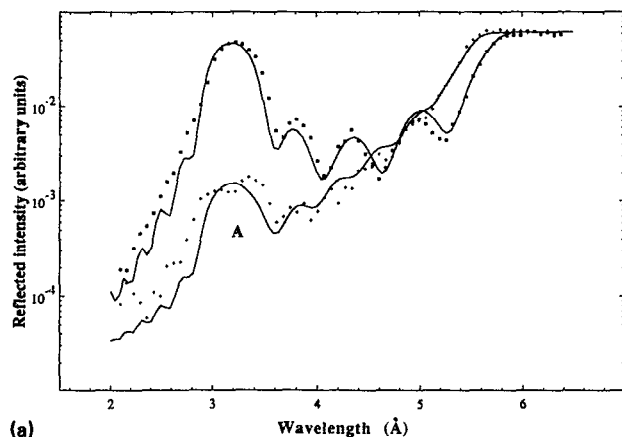
FIG. 3. (a) Modelling of interfacial roughness by replacing the "ideal" superlattice repeat until A by a repeat until B that includes buffer layers of mixed composition at each interface. (b) To simulate the effects of surface oxidation and roughness, the topmost "ideal" cobalt layer A is replaced by B which includes a cobalt oxide layer together with buffer layers of mixed composition at each interface.

of the incident neutron beam. A depolarization of as little as a few percent could be significant in regions where the difference between spin-parallel and spin-antiparallel neutron reflectivities is large; for example, it could significantly affect the measured spin-parallel reflectivity at the superlattice diffraction condition [below peak A in Fig. 2(b)].

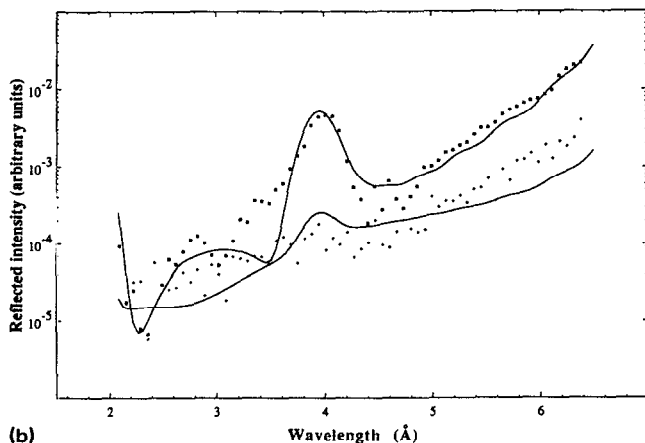
The fully refined calculations for sample C146, including effects due to interfacial roughness and allowing for a 3% depolarization in the incident beam, are shown in Fig. 4(a). The fit to the experimental data in the region between the critical edge and the spin-antiparallel diffraction peak is a considerable improvement over that shown in Fig. 2. It is particularly important to include the effects of surface oxidation when the scattering density of the oxide differs significantly from that of the metal, as in the present system. Although the agreement between data and calculation is improved by including roughness and oxidation, it is not possible to make fine distinctions between equally good fits obtained with different values of the roughness parameters. In this sense, the thickness of the buffer layers is not determined as reliably as the basic structural and magnetic quantities that derive from the position of the diffraction peaks.

Figure 4(b) shows the reflectivities measured for the same sample (C146) with a higher angle of incidence ( $\sim 1.0^\circ$ ). The curves are calculated with the same model as in Fig. 4(a) and with no change in the structural parameters. The large spin-antiparallel peak is the second-order diffraction peak corresponding to the superlattice periodicity. As may be seen from the figure, the calculations still give a good fit to the experimental data even though the use of a single buffer layer to represent the interfacial roughness is likely to be less effective in describing the higher-order diffraction peaks than the lower-order peaks.

A similar model was used to fit the reflectivity profiles from sample C29, which has a smaller superlattice repeat distance. Data for this sample are shown in Fig. 5, together with the calculated intensities. Figure 5(a) gives the data



(a)

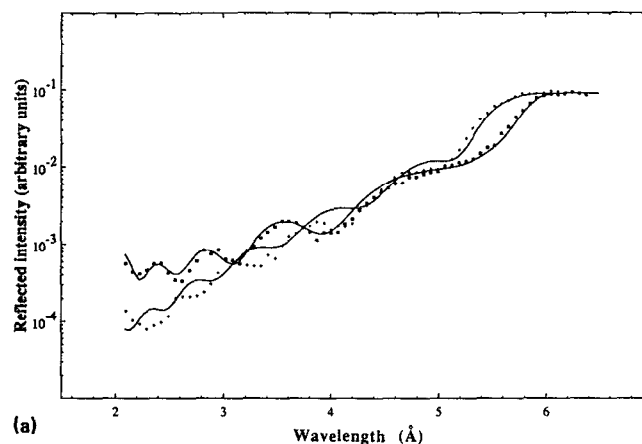


(b)

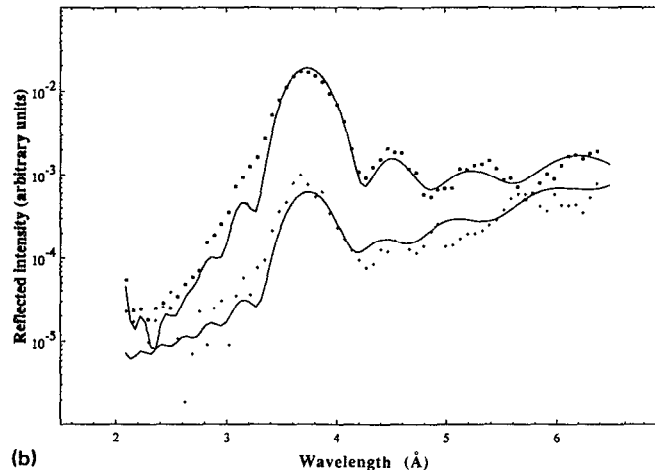
FIG. 4. (a) The measured neutron reflectivities for spin-parallel (crosses) and spin-antiparallel (squares) configurations with sample C146 (nominally eight repeat units of 146 Å copper and 72 Å cobalt). The curves are the reflectivities calculated with a model that includes buffer layers to represent interfacial roughness and surface oxidation. In addition, 3% of the spin-antiparallel reflectivity was added to the calculated spin-parallel reflectivity to compensate for possible beam depolarization. To improve the fit still further,  $m$  was slightly reduced (to  $1.6 \mu_B$ ) while the effective angular resolution was slightly increased. The thickness of the cobalt-copper buffer layers was 42 Å, the thickness of the top cobalt layer was 7 Å, the thickness of the cobalt/cobalt oxide buffer layers was 56 Å, the thickness of the cobalt oxide layer was 55 Å, and the thickness of the cobalt oxide/air buffer layer was 12 Å. (b) Measured and calculated neutron reflectivities for sample C146 at  $1.0^\circ$  angle of incidence. The calculated intensities used the same structural parameters as in (a).

at an angle of incidence of approximately  $0.45^\circ$  and shows the critical edge clearly. Figure 5(b) is for a larger angle of incidence ( $1.0^\circ$ ) where the first-order diffraction peak from the superlattice is the most prominent feature. In both cases the agreement between the calculated reflectivities and the experiment is good.

The buffer layer thicknesses used to fit the C29 data were somewhat smaller than for sample C146, as was the oxide thickness, but since it was possible to vary these thicknesses and still obtain quite a good fit to the data, the error in the buffer-layer/oxide-layer thicknesses could be as high as 50% for both samples. Interestingly, it was again necessary to decrease the density of the film ( $\rho_{Cu}$  and  $\rho_{Co}$ ) relative to the bulk values in order to obtain a good fit to the data.



(a)



(b)

FIG. 5. (a) The measured neutron reflectivities for spin-parallel (crosses) and spin-antiparallel (squares) configurations with sample C29 (nominally eight repeat units of 29 Å copper and 73 Å cobalt) for  $\sim 0.45^\circ$  angle of incidence. The solid lines are the reflectivities calculated for cobalt and copper thicknesses 5% greater than the nominal thicknesses and densities 5% lower than the bulk values. The average magnetic dipole moment per cobalt atom was  $1.7 \mu_B$ . 3% of the spin-antiparallel reflectivity was added to the calculated spin-parallel reflectivity to compensate for possible beam depolarization. The thickness of the cobalt-copper buffer layers was 7 Å, the thickness of the top cobalt layer was 43 Å, the thickness of the cobalt/cobalt oxide buffer layer was 33 Å, the thickness of the cobalt oxide layer was 20 Å, and no cobalt oxide/air buffer layer was needed. (b) Measured and calculated neutron reflectivities for sample C29 at  $1.0^\circ$  angle of incidence. The calculated intensities used the same structural parameters as in (a).

## V. CONCLUSION

This experiment has shown that polarized neutron reflection is a useful technique for the characterization of magnetic multilayers. In particular, the critical edge positions are sensitive to the average scattering density and magnetization of the film, while the superlattice diffraction peaks are sensitive to the repeat distance. Interfacial roughness and surface oxidation affect the fine structure in the data.

For the two cobalt/copper superlattice samples that we have measured, the position of both the spin-antiparallel diffraction peak and the spin-parallel critical edge lead to the conclusion that, while the density of the

sputtered films are approximately 5% less than the bulk material, the cobalt magnetic dipole moment is little changed compared to the bulk. In addition the reflectivity data showed significant oxidation of the top cobalt layer for both samples.

## ACKNOWLEDGMENTS

One of us (W.S.) wishes to acknowledge the award of a research studentship by the Department of Education and Science for Northern Ireland and financial support from Emmanuel College, Cambridge.

<sup>1</sup>G. P. Felcher, Phys. Rev. B **24**, 1595 (1981).

<sup>2</sup>T. Katayama, H. Awano, and Y. Nishihara, J. Phys. Soc. Jpn. **55**, 2539 (1986).

<sup>3</sup>M. N. Baibich, J. M. Broto, A. Fert, F. Nguyen Van Dau, F. Petroff, P. Etienne, G. Creuzet, A. Friederich, and J. Chazelas, Phys. Rev. Lett. **61**, 2472 (1988).

<sup>4</sup>G. Binasch, P. Grünberg, F. Saurenbach, and W. Zinn, Phys. Rev. B **39**, 4828 (1989).

<sup>5</sup>M. Sato, K. Abe, Y. Endoh, and J. Hayter, J. Phys. C **13**, 3563 (1980).

<sup>6</sup>G. P. Felcher, J. W. Cable, J. Q. Zheng, J. B. Ketterson, and J. E. Hilliard, J. Magn. Magn. Mater. **21**, L198 (1980).

<sup>7</sup>C. F. Majkrzak, Physica B **156&157**, 619 (1989).

<sup>8</sup>C. F. Majkrzak, J. D. Axe, and P. Böni, J. Appl. Phys. **57**, 3657 (1985); C. F. Majkrzak, Physica B **136**, 69 (1986).

<sup>9</sup>C. M. Falco, W. R. Bennett, and A. Boufelfel, in *Dynamical Phenomena at Surfaces, Interfaces and Superlattices*, edited by F. Nizzoli, K. H. Rieder, and R. F. Willis (Springer, Berlin, 1985), p. 35.

<sup>10</sup>C. D. England, W. R. Bennett, and C. M. Falco, J. Appl. Phys. **64**, 5757 (1988).

<sup>11</sup>O. S. Heavens, *Optical Properties of Thin Films* (Butterworths, London, 1955).

<sup>12</sup>J. Penfold, R. C. Ward, and W. G. Williams, J. Phys. E **20**, 1411 (1987); R. Felici, J. Penfold, R. C. Ward, and W. G. Williams, Appl. Phys. A **45**, 169 (1988).

<sup>13</sup>T. J. L. Jones and W. G. Williams, Nucl. Instrum. Methods **152**, 463 (1978).

<sup>14</sup>L. Nénot and P. Croce, Rev. Phys. Appl. **15**, 761 (1980).

<sup>15</sup>W. Schwarzacher, Ph.D. thesis, University of Cambridge, 1990.

<sup>16</sup>A. Bogen and J. Küppers, Surf. Sci. **134**, 223 (1983).

<sup>17</sup>B. W. Lee, A. Ignatiev, J. A. Taylor, and J. W. Rabelais, Solid State Commun. **33**, 1205 (1980).